Temperature characteristics of hot electron electroluminescence in silicon

Monuko du Plessis,[1,*] Hanqing Wen,[2] and Enrico Bellotti[2]

[1] *Carl and Emily Fuchs Institute for Microelectronics, University of Pretoria, Pretoria 0002, South Africa*
[2] *Electrical and Computer Engineering Department, Boston University, 8 Saint Mary's St., Boston, MA 02215, USA*
[*] monuko@up.ac.za

Abstract: Emission spectra of avalanching n^+p junctions manufactured in a standard CMOS technology with no process modifications were measured over a broad photon energy spectrum ranging from 0.8 eV to 2.8 eV at various temperatures. The temperature coefficients of the emission rates at different photon energies were determined. Below a photon energy of 1.35 eV the temperature coefficient of emission was positive, and above 1.35 eV the temperature coefficient was negative. Two narrowband emissions were also identified from the temperature characterization, namely an enhanced positive temperature coefficient at 1.15 eV photon energy, and an enhanced negative temperature coefficient at 2.0 eV. Device simulations and Monte Carlo simulations were used to interpret the results.

References and links

1. A. R. Chen, A. I. Akinwande and H-S. Lee, "CMOS-based microdisplay with calibrated backplane," IEEE J Solid-State Circuits **40**(12), 2746–2755 (2005).
2. M. du Plessis, H. Aharoni and L.W. Snyman, "Spatial and intensity modulation of light emission from a silicon LED matrix," IEEE Photon. Technol. Lett. **14**(6), 768–770 (2002).
3. P. J. Venter and M. du Plessis, "A 128x96 pixel CMOS microdisplay utilizing hot carrier electroluminescence from junctions in reach through," J. Disp. Technol. **10**(9), 721–728 (2014).
4. M. Lahbabi, M. Jorio, A. Ahaitouf, M. Fliyou and E. Abarkan, "Temperature effect on electroluminescence spectra of silicon p-n junctions under avalanche breakdown condition," Mater. Sci. Eng. B **86**, 96–99 (2001).
5. H. Elghazi, A. Jorio and I. Zorkani, "Analysis of temperature and 1 MeV proton irradiation effects on the light emission in bulk silicon (npn) emitter-base bipolar junctions," Opt. Commun. **280**, 278–284 (2007).
6. L. Selmi, M. Mastrapasqua, D. M. Boulin, J. D. Bude, M. Pavesi, E. Sangiorgi and M. R. Pinto, "Verification of electron distributions in silicon by means of hot carrier luminescence measurements," IEEE Trans. Electron. Dev. **45**(4), 802–808 (1998).
7. K. Xu, "Electro-optical modulation processes in Si-PMOSFET LEDs operating in the avalanche light emission mode," IEEE Trans. Electron. Dev. **61**(6), 2085–2092 (2014).
8. M. du Plessis, P. J. Venter and E. Bellotti, "Spectral characteristics of hot electron electroluminescence in silicon avalanching junctions," IEEE J. Quantum Electron. **49**(7), 570–577 (2013).
9. Sentaurus Device User Guide (Synopsys, Version G-2012.06, June 2012), www.synopsys.com.
10. R. Quaya, C. Moglestue, V. Palankovski and S. Selberherr, "A temperature dependent model for the saturation velocity in semiconductor materials," Mater. Sci. Semicond. Process. **3**(1-2), 149–155 (2000).
11. L. Tirino, M. Weber, K. F. Brennan and E. Bellotti, "A general Monte Carlo model including the effect of the acoustic deformation potential on the transport properties," J. Comput. Electron. **3**(2), 81–93 (2005).
12. J. Bude, N. Sano and A. Yoshii, "Hot carrier luminescence in Si," Phys. Rev. B **45**(11), 5848–5856 (1992).
13. K. Xu and G. P. Li, "A novel way to improve the quantum efficiency of silicon light-emitting diode in a standard silicon complementary metal–oxide–semiconductor technology," J. Appl. Phys. **113**, 103106 (2013).
14. S. Tam, F-C. Hsu, C. Hu, R. S. Muller and P. K. Ko, "Hot-electron currents in very short channel MOSFET's," IEEE Electron Device Lett. **4**(7), 249–251 (1983).
15. J. Yuan and D. Haneman, "Visible electroluminescence from native SiO_2 on n-type Si substrates," J. Appl. Phys. **86**(4), 2358-2360 (1999).
16. L. Heikkilä, T. Kuusela and H.-P. Hedman, "Electroluminescence in Si/SiO_2 layer structures," J. Appl. Phys. **89**(4), 2179–2184 (2001).
17. A. M. Emel'yanov, N. A. Sobolev, T. M. Mel'nikova and S. Pizzini, "Efficient silicon light-emitting diode with temperature-stable spectral characteristics," Semiconductors **37**(6), 730–735 (2003).

1. Introduction

CMOS based light sources have been shown to exhibit illumination levels that can be utilized in micro displays [1–3]. In these micro display applications the wide operational temperature range of the CMOS based avalanche electroluminescent micro display devices is cited as a distinct advantage compared to the well-established LCD and OLED technologies.

The effect of temperature on the spectral characteristics of avalanching pn junctions in silicon has been studied in theory [4], with emphasis on emissions of photons with energies higher than 1.5 eV. The conclusion was that as the operating voltage increases with increasing temperature (the avalanching breakdown voltage has a positive temperature coefficient), the electric field inside the junction will also increase. The electron energy will then depend on both the mean free path (m.f.p.) of the electron–phonon interaction and the electric field. These two effects vary in the opposite sense with temperature. That is, at decreasing temperature, the electric field limits the effect of the m.f.p. increase on the emitted light intensity. It could not be shown whether the two opposite effects will result in a positive or negative temperature coefficient for the photon rate of emission, but theoretical calculations using an interband recombination model resulted in a small positive temperature coefficient (TC) of + 0.12 %/K for the light emission intensity for the case where the internal electric field effect is taken into account.

Experimental characterization of the spectral properties of photon emission with energies in excess of 1.5 eV from avalanching silicon pn junctions as a function of temperature was performed some time later [5]. The measured negative temperature coefficient for the light intensity at 300K was in the order of − 0.38 %/K, in contrast to the previous theoretical prediction. Instead of avalanching pn junctions, the light emission from an n^+nn^+ structure was measured and simulated, with the electric field falling mostly across the central n-type region [6]. In this case the negative TC for photon energy radiation more than 1.5 eV was in the range of − 0.7 %/K. Experimental data indicated that the temperature coefficient will be less negative at higher electric fields. Since the average electric field in the devices tested was 150 kV/cm [6], it can be expected that the temperature coefficient in our pn junction device will be less negative since the electric field is significantly larger in avalanching junctions [7].

In this paper the conflicting results of the above theoretical and empirical approaches described are investigated, as well as TC properties of photon emission of photons with energies less than 1.5 eV. We use spectral measurements, combined with Monte Carlo and device simulations, to investigate the effect of temperature on the silicon avalanche electroluminescent device spectral characteristics.

2. Device design

The pn junctions under investigation were designed and manufactured in the standard *ams* 0.35 μm CMOS process without any post-processing. The layout and cross section of a single point source test device are shown in Fig. 1. To achieve higher levels of optical power being emitted, 400 identical point sources were connected in parallel to form an array. The nominal test current was 140 mA, with 350 μA flowing in each point source at 10.5 V bias. This bias current results in a current density J = 500 kA/cm^2 in the device.

3. Experimental procedure

The output spectra of the array of 400 point sources were measured using two different spectrometers, namely a Si UV-Vis-NIR spectrometer (Avantes AvaSpec 2048TEC) covering the range 450 nm to 1100 nm, and an InGaAs NIR spectrometer (B&WTEK SOL 1.7) that covered the wavelength range 900 nm to 1700 nm. From the known relative responses of the two spectrometers, as well as their overlapping spectral ranges, the two spectra could be merged into one externally observed spectrum. From these measured spectra, the photon emission rates at the light generation site within the silicon were determined by taking the

interference patterns of the Si-oxide-air interface, critical angles of internal reflection and substrate absorption effects into account.

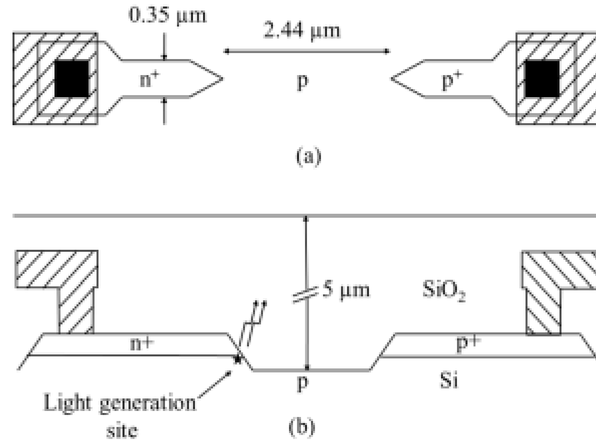

Fig. 1. (a) Layout design, and b) cross section of CMOS n^+p point source.

The test devices were heated on a temperature controlled hot plate to perform measurements at different junction temperatures. A good indication of the junction temperature was achieved by measuring the current vs. voltage (I-V) characteristics of a forward biased pn junction in close proximity to the array of light sources on the same chip. This reference forward biased diode I-V curve was separately calibrated versus its own junction temperature in a temperature controlled oven. Using the calibrated I-V values of this reference, its junction temperature could be accurately monitored on the chip during testing. It is assumed that the light source array junction temperature will be very close to that of the calibrated reference junction in this experimental procedure. Since the measurements were quite time consuming only one sample was measured in detail followed by some spot checks using a second sample to verify the temperature coefficient values.

4. Experimental results

The emission spectra at constant reverse bias current were determined in the temperature range 22°C to 122°C. In many cases different physical mechanisms can be discriminated more easily by measuring the effect of junction temperature on the device performance. The results for the three temperatures 22°C, 77°C and 122°C are shown in Fig. 2. Examining Fig. 2, it is evident that two different temperature dependencies are observed. At low energies there is a positive TC, and at higher energies there is a negative TC, with 1.35 eV the zero temperature coefficient cross-over photon energy. Furthermore, a distinct narrowband attenuation in emission at 2.0 eV photon energy is observed at the higher temperature. In contrast, the photon generation at 1.15 eV is enhanced significantly when the temperature is increased.

The temperature effects can be better evaluated by plotting the relative temperature responses of emissions at a number of relevant photon energies, normalized to the emission at 40ºC. The result is shown in Fig. 3 where an approximate linear temperature response is seen for all photon energies, except for the 2.0 eV photon energy emission. Up to a junction temperature of 90°C the 2.0 eV emission temperature response is identical to that of the wideband emission above 1.35 eV photon energy, but at higher temperatures the 2.0 eV emission exhibits an enhanced negative temperature coefficient. This is an indication of an increase in narrowband photon absorption at 2.0 eV, probably in the silicon dioxide layer or at the Si-oxide interface.

Assuming a linear temperature response, the temperature coefficient (TC) was determined as a function of photon energy from the slopes of the normalized curves in Fig. 3. The TC as a function of photon energy is shown in Fig. 4. At the photon energy of 1.35 eV the TC changes sign. At energies below this value, the TC is positive with a value of approximately + 0.5 %/K, and above this energy level of 1.35 eV the TC is negative with a value of approximately − 0.25 %/K. Also very much in evidence in Fig. 4 is a narrowband emission near 1.15 eV, only observed by an enhanced positive temperature coefficient. This is very close to the bandgap energy of silicon (1.12 eV) and is most probably due to the indirect interband band edge recombination of carriers in the drift region of the device where relatively low electric fields are present.

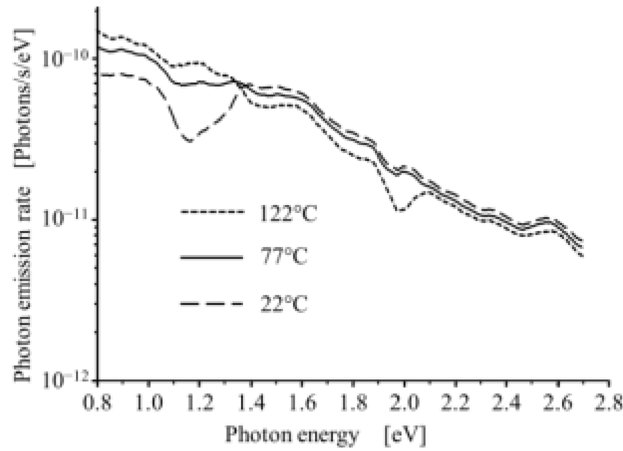

Fig. 2. The measured photon emission spectrum at three junction temperatures.

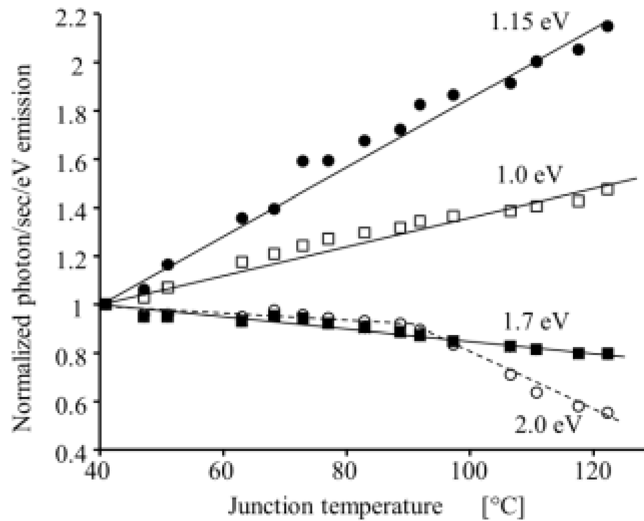

Fig. 3. The normalized temperature response of photon emission.

From the TC graph in Fig. 4, four mechanisms can now be identified, namely i) a wideband emission dominant below 1.35 eV with a positive TC, and ii) another wideband emission dominant above 1.35 eV with a negative TC, and iii) a narrow band emission at

1.15 eV with positive TC, and lastly iv) a narrowband attenuation at 2.0 eV with negative TC and only observed at a junction temperature above 90ºC.

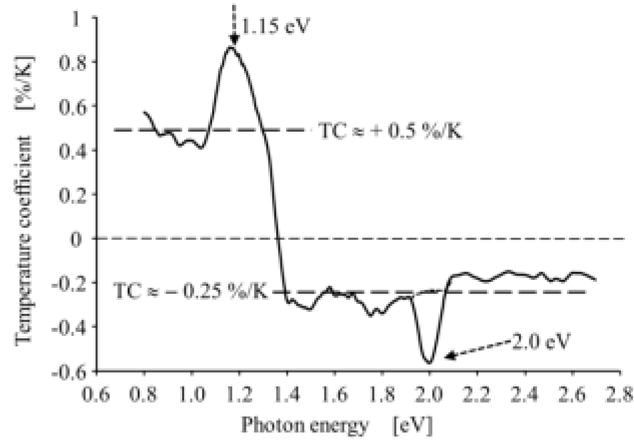

Fig. 4. The measured temperature coefficient (TC) of photon emission.

5. Simulation results

5.1 Electric field and electron concentration

With device simulation [8,9] the electric field and electron concentration within the device could be determined as a function of temperature. The results are shown in Fig. 5. In this figure, two distinct regions within the device can be identified, namely i) the high electric field region where avalanching is taking place with an electric field in the region of 600 kV/cm, and ii) the lower electric field drift region with average electric field close to 200 kV/cm. Although the bias current is kept constant with the increase in temperature, the increase in temperature resulted in an increase in both the spatial electron concentration n and the internal electric field E throughout the device with the same positive TC of + 0.15 %/K. Furthermore, the electron concentrations in the two regions of the device are fairly close in value.

The electron current density J_n in the device is given by $J_n = nqv$, with n = electron concentration, q = electron charge and v = carrier drift velocity. In the avalanche mode of operation where the electric field is quite high, the carrier drift velocity will approach the saturation carrier velocity, which is a weak function of electric field. During the simulation (and measurement) the current density was kept constant and it then follows that the product nv must remain constant with changing temperature. It is well known that with increasing temperature, the electric field will increase in the avalanche region of operation [4]. The drift velocity v is a very weak function of electric field at high field strengths, but the carrier saturation velocity has been shown to have a negative temperature coefficient [10]. Thus the carrier concentration n will increase with increasing temperature to counter the effect of reduced carrier velocity v. The device simulation results of Fig. 5 show the positive temperature coefficients of the electric field E and the carrier concentration n as was expected from this analysis.

5.2 Hot electron energy distribution (EED)

To evaluate the EED within the conduction band in the two device regions, Monte Carlo simulations [8,11] were performed at the two electric fields. The EED function can be derived from the density of states function and the probability distribution function of electrons. The simulation results are shown in Fig. 6.

The simulated EED plots in Fig. 6 emphasize the difference in electron distribution between the two regions of low and high electric field. From this result it can be postulated that photons with energy above 1.35 eV will be generated mostly in the high electric field avalanching region, while the photons with energy below 1.35 eV will mostly be generated in the low electric field drift region.

Both Fig. 2 and Fig. 6 exhibit a cross over between curves at the photon energy of 1.35 eV (Fig. 2) and electron energy of 1.35 eV (Fig. 6) respectively. Since the dominant photon generating mechanism in the device has been previously identified as intraband direct and indirect electron transitions, it can be expected that there will be a close correlation between photon and electron energy since in intraband transitions the energy lost by an electron transition will be emitted in the form of a photon, albeit with a low quantum efficiency.

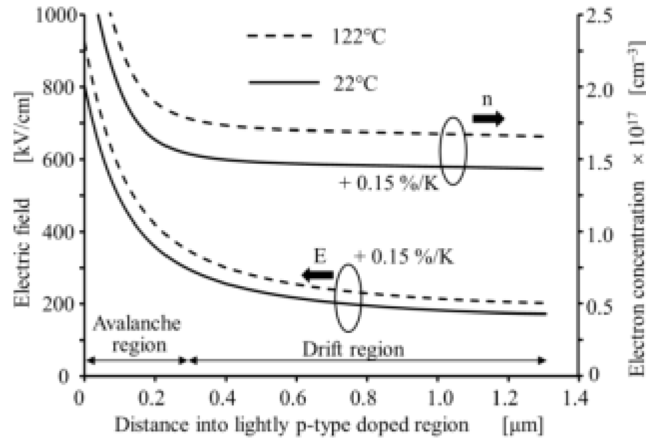

Fig. 5. Simulated electric field E and electron concentration n as a function of temperature and position in the device.

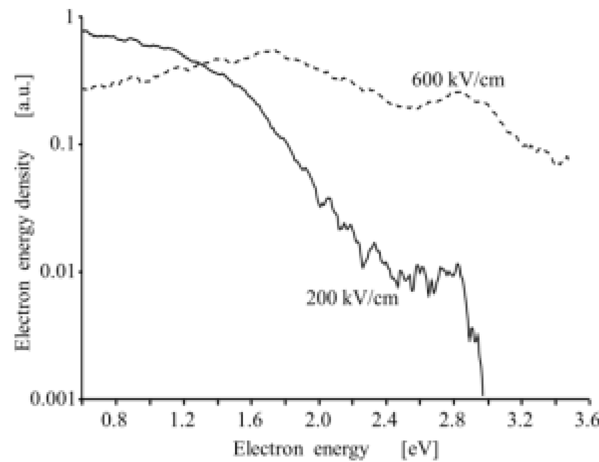

Fig. 6. Monte Carlo simulated electron energy distribution EED.

6. Discussion of results

The dominant electronic process generating photons in a silicon reverse biased junction has previously been postulated to be intraband c-c (conduction-to-conduction band) electron relaxation processes. This was done both experimentally [6] and by simulation [6,12].

From the measured emission spectra of silicon hot electron electroluminescent devices, it is not that easy to identify the photon generating mechanisms taking place, and thus several models have been proposed over the years to fit the experimental and simulated data.

The dominant intraband c-c photon generating process can be either a direct c-c or an indirect phonon assisted (PA) c-c transition. It was found by simulation that the direct c-c radiation dominates at lower photon energies, and the indirect PA c-c radiation dominates at higher energies [6,12]. A detailed theoretical study was made of the relationship between the kinetic energy of a carrier, the effective carrier temperature, and the corresponding photon distribution assuming an exponential distribution of hot-carriers in the conduction band [13].

Using the simulation data [6] and the empirical relationship [14] between effective electron temperatures T_e and electric field E ($T_e = 9.05\times10^{-3}\times E$), it can be derived that at $T_e = 1\,700$K (estimate E = 188 kV/cm) the crossover energy between the two mechanisms is 1.26 eV. The crossover energy increases slightly with increasing electric field. This is very close to our measured crossover energy of 1.35 eV at higher electric fields.

It should be noted that electroluminescence from defects and states at or near the Si/SiO_2 interface have been observed to emit a wideband spectrum as well, peaking near a photon energy of 1.9 eV [15,16]. These results were, however, very much dependent on the specific device structure and materials, as well as processing technique. This light emission from defects has not in general been considered as the dominant mechanism for photon generation in avalanching junctions.

6.1 Wideband emission above 1.35 eV photon energy

It has been shown that the majority of the photons being emitted above 1.35 eV photon energy will be in the high electric field avalanching region of the device where the electric field is approximately 600 kV/cm. Comparing the photon emission spectra in Fig. 2 with the EED graph of Fig. 6, especially looking at the slopes of the curves, one can postulate that the photon emission is due to intraband carrier transitions. In the case of phonon assisted (PA) indirect transitions at higher photon energies, as the temperature increases, the mean free path of electron-phonon interaction decreases. The phonon scattering is thus increased and leads to less energetic electrons. Consequently, the emitted light intensity decreases, resulting in a negative TC. Taking only the effect of mean free path into account, the photon emission at energies in excess of 1.4 eV was calculated to be in the order of − 1.4 %/K [4]. The positive TC of the electric field and carrier concentration (see Fig. 5) will cause the experimentally observed TC to have a less negative value. Indeed, in our case the wideband emission above 1.35 eV has a TC of − 0.25 %/K. This negative TC is an indication that the photon generation is mostly due to intraband PA indirect transitions at photon energies in excess of 1.35 eV.

The three photon generation mechanisms identified in this study is shown in Fig. 7. The two wideband intraband transition phenomena (direct c-c for photon energies less than 1.35 eV, and the indirect c-c for photon energies more than 1.35 eV) are shown within the conduction band of the device. The narrowband interband indirect recombination process (indirect c-v at about 1.15 eV) is also indicated in the figure.

6.2 Wideband emission below 1.35 eV photon energy

The photon energies in this band include values less than the band gap energy of silicon, thus the photon generation can only be intraband in this spectral band. At photon energies below 1.35 eV the wideband emission exhibits a fairly large positive TC of + 0.5 %/K. This means that the negative TC effect of the mean free path of electron-phonon interaction is not present, but only the positive TC effect of the increase in electric field and carrier concentrations. These emissions are then mostly direct intraband transitions.

6.3 Narrowband emission at 1.15 eV photon energy

This emission is a fairly narrow emission near the band gap energy of silicon. Since band-to-band recombination at this energy level can only be indirect, this emission will be an interband c-v indirect recombination process. It is known that the internal quantum efficiency of the band-to-band emission can be defined by the ratio of the minority carrier lifetime of carriers τ_p to the radiative lifetime τ [17]. The lifetime of minority charge carriers τ_p is mainly controlled in silicon by nonradiative recombination. The temperature dependence of the light intensity at a fixed value of current is governed by the temperature dependences of τ_p and τ. In a study the dependence of τ_p on temperature at a constant current level was measured and found to have a positive TC at room temperature [17], eventually resulting in a positive TC for band-to-band indirect recombination. It can thus be concluded that the narrowband emission at 1.15 eV is due to interband indirect band-to-band recombination.

6.4 Narrowband attenuation at 2.0 eV photon energy

This narrowband attenuation at 2 eV was only observed above 90ºC and the origin and temperature behavior of this anomaly requires further investigation.

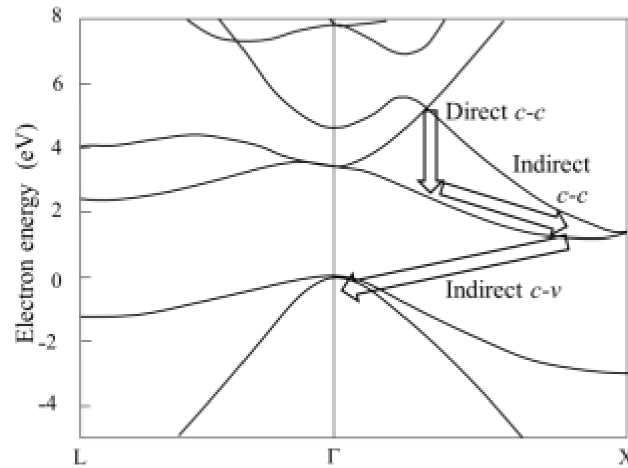

Fig. 7. The band structure of silicon showing three radiative mechanisms.

7. Conclusions

In this study we have shown that by measuring the effect of temperature on the emission spectrum of silicon junctions in avalanche breakdown, several photon generating mechanisms could be identified. For wideband emissions above 1.35 eV photon energy the negative temperature coefficient is due to intraband phonon assisted indirect transitions, and at lower energies the positive temperature coefficient is due to direct intraband transitions. The higher positive temperature coefficient narrowband emission near 1.15 eV photon energy is due to band edge interband indirect carrier recombination.

Acknowledgments

The work at the University of Pretoria was financially supported in part by INSiAVA (Pty) Ltd., Pretoria, South Africa. The work at Boston University was supported in part by the U.S. Army Research Laboratory through the Collaborative Research Alliance (CRA) for MultiScale multidisciplinary Modeling of Electronic materials (MSME).